Polymer Journal, Vol. 37, No. 12, pp. 932–938 (2005)

Nonisothermal Crystallization of Compatible PCL/PVC Blends under Supercritical CO_2

Yeong-Tarng SHIEH,[1,†] Huang-Shung YANG,[1] Hsin-Lung CHEN,[2] and Tsang-Lang LIN[3]

[1]*Department of Chemical Engineering, National Yunlin University of Science and Technology, Touliu, Yunlin 640, Taiwan, R.O.C.*
[2]*Department of Chemical Engineering, National Tsing Hua University, Hsin-Chu 300, Taiwan, R.O.C.*
[3]*Department of Engineering and System Science, National Tsing Hua University, Hsin-Chu 300, Taiwan, R.O.C.*

(Received May 9, 2005; Accepted August 19, 2005; Published December 15, 2005)

ABSTRACT: Nonisothermal crystallizations of polycaprolactone (PCL) in the presence of poly(vinyl chloride) (PVC) at a cooling rate of 0.5 °C/min from 90 to 30 °C under supercritical CO_2 at a constant pressure 304 atm were investigated. DSC and SAXS data found that the nonisothermal crystallizations of the PCL/PVC blends under supercritical CO_2 resulted in decrease in thickness of the crystalline layers in the lamellar stacks. These nonisothermal supercritical CO_2 treatments also generated a morphological heterogeneity with size (13.8 nm for pure PCL) larger than the long period (12.1 nm) of the lamellar stacks. The size of this heterogeneity was slightly enhanced from 13.8 nm for pure PCL to 15.2 and 16.3 nm for the blends containing 10 and 25 wt % PVC, respectively.
[DOI 10.1295/polymj.37.932]

KEY WORDS Polycaprolactone / Poly(vinyl chloride) / Supercritical CO_2 Fluid / Crystallization / DSC / SAXS /

Supercritical CO_2 fluids or compressed CO_2 gases or liquids have drawn much attention because the environmentally friendly carbon dioxide (especially the supercritical CO_2) is a potential candidate to be an alternative to substitute for organic chemicals used in synthesis,[1–3] modification and processing of polymers as was recently reviewed.[4] Polymers subjected to the supercritical CO_2 fluids may result in melting temperature depressions,[5,6] phase separations,[7] or morphological changes.[5,8–10] Since crystallization of a polymer leads to a morphology that can determine its final physical properties, it is important to reveal the crystallization behavior of the polymer under supercritical CO_2 fluids before these fluids can be practically used for processing of the polymer.

Poly(ε-caprolactone) (PCL) is a crystalline and biodegradable aliphatic polyester having a glass transition temperature of about −60 °C and a melting temperature of about 60 °C. In a previous study,[10] we investigated the morphological changes of PCL under isothermal (35 °C) high-pressure (36, 84, and 304 atm) CO_2 treatments by means of DSC and SAXS. It was found that PCL melted under 84 and 304 atm of CO_2 at 35 °C, a much lower temperature than T_m of PCL. The CO_2-assisted melting of PCL recrystallized during depressurization of CO_2, resulting in a varied thickness of crystal layers and amorphous layers with CO_2 pressures. This report presents a continuing study of our previous work.[10] This work aims at the nonisothermal crystallization behavior of PCL under supercritical CO_2 at a constant pressure 304 atm at a cooling rate of 0.5 °C per min from 90 °C to 30 °C in the presence of various amounts of PVC. It will be seen from DSC and SAXS data that the nonisothermal crystallizations of the PCL/PVC blends under supercritical CO_2 result in decrease in thickness of crystalline layers of the lamellar stacks. Heterogeneity, with a size larger than the long period, is formed after nonisothermal crystallizations under supercritical CO_2. The size of this heterogeneity is found to slightly increase with increasing PVC contents.

EXPERIMENTAL SECTION

Materials and Sample Preparations

Polycaprolactone (PCL) pellets with $M_n = 80{,}000$ were acquired from Aldrich Chemical Company. Poly(vinyl chloride) (PVC), prepared by a suspension polymerization with a degree of polymerization of about 1000 and with a product number S-65, was supplied by Formosa Plastics Corporation (Taipei, Taiwan). Specimens of *ca.* 1.3 mm in thickness of the blends were prepared by dissolving 0.4 g of the blends in 20 mL tetrahydrofuran, followed by casting and drying at room temperature for one week. The specimens were then subjected to nonisothermal supercritical CO_2 treatments at a constant pressure 304 atm at a cooling rate of 0.5 °C/min from 90 to 30 °C, as described below.

[†]To whom correspondence should be addressed (Tel: +886-5-534-2601, Fax: +886-5-531-2071, E-mail: shiehy@yuntech.edu.tw).

Nonisothermal Supercritical CO_2 Treatments

The CO_2 treatments were performed in a supercritical extractor supplied by ISCO (Lincoln, Nebraska) with a model SFX 2–10 which was equipped with a syringe pump with a model 260D. The polymer specimens were put in a 10-cm^3 cell located inside the extractor pressurized by the equipped syringe-type pump. For the nonisothermal crystallization of a sample under supercritical CO_2, the sample was heated inside the cell and held at 90 °C for 60 min at 304 atm. The melted sample was then cooled to 30 °C under the 304-atm CO_2 at a rate of 0.5 °C per min to conduct the nonisothermal crystallization. After holding at 30 °C for 24 h, the cell was depressurized at a controlled constant volumetric flow rate to ambient pressure and the sample was taken out for DSC measurements. A sample prepared in the same way as above except the presence of CO_2 was used as the control sample for comparison. The samples after the CO_2 treatments and complete evacuation of the CO_2 inside the samples by a vacuum heating showed a negligible weight change, indicating that neither CO_2 resided inside the samples nor any part of the samples was dissolved away.

DSC Measurements

The melting temperatures, heats of fusion, and crystallinities of samples after nonisothermal crystallizations under 304 atm-CO_2 were measured by differential scanning calorimeter (DSC 2010) of TA Instruments (New Castle, DE) from the first heating scan from −10 to 90 °C at a heating rate of 10 °C per min. The weight fractional bulk crystallinity (ω_c) was determined by dividing the heat of fusion, ΔH, in J/g of a sample by ΔH°, which is 142 J/g for perfectly crystalline PCL.[11] For Figure 1, the samples were first heated at 10 °C/min, followed by cooling and heating again at the same rate.

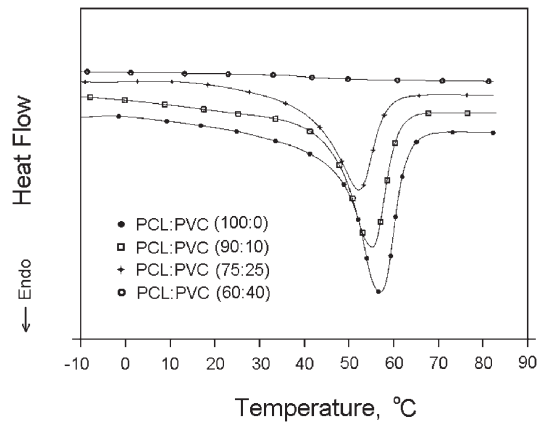

Figure 1. DSC melting curves obtained from the second heating scans for the PCL/PVC blends before CO_2 treatments.

DMA Measurements

The dynamic mechanical properties of samples were investigated by the dynamic mechanical analyzer (DMA, TA Instruments, DMA 2980) for rectangular specimens. The DMA was measured in the tensile mode at a constant frequency of 1 Hz and a heating rate of 3 °C per minute scanning from −80 to 50 °C.

SAXS Measurements

All SAXS measurements were performed at room temperature. The X-ray source was operated at 200 mA and 40 kV and was generated by an 18 kW rotating anode X-ray generator (Rigaku) with a rotating anode Cu target. The incident X-ray beam was monochromated by a pyrolytic graphite and a set of three pinhole inherent collimators was used so that the smearing effects inherent in slit-collimated small-angle X-ray cameras can be avoided. The sizes of the first and second pinhole are 1.5 and 1.0 mm, respectively, and the size of the guard pinhole before the sample is 2.0 mm. The scattered intensity was detected by a two-dimensional position sensitive detector (Ordela Model 2201X, Oak Ridge Detector Laboratory Inc.) with 256 × 256 channels (active area 20 × 20 cm^2 with ∼1 mm resolution). The sample to detector distance is 4000 mm long. The beam stop is around lead disk of 18 mm in diameter. All data were corrected by the background (dark current and empty beam scattering) and the sensitivity of each pixel of the area detector. The area scattering pattern has been radially averaged to increase the efficiency of data collection compared with one-dimensional linear detector. Data were acquired and processed on an IBM-compatible personal computer. The intensity profile was output as the plot of the scattering intensity (I) as a function of the scattering factor, $q = (4\pi/\lambda)(\sin(\theta/2))$ (θ = scattering angle).

RESULTS AND DISCUSSION

Figure 1 shows DSC melting curves obtained from the second heating scans for the PCL/PVC blends before CO_2 treatments. As can be seen in Figure 1, the melting temperature of PCL was about 57.5 °C and was depressed by the presence of PVC. The depression of melting temperature of PCL increased with increasing PVC contents until 40 wt % at which crystallization of PCL was not observed by DSC measurements. The crystalline PCL/PVC blends (100/0, 90/10, and 75/25) are thus chosen to investigate the nonisothermal crystallizations under supercritical CO_2 at 304 atm. The melting temperature depression in the PCL/PVC blends suggested that specific interactions were present between PCL and PVC,[12] which resulted in miscible PCL/PVC amorphous domain as indicated

Table I. The melting temperatures (T_m, °C), heats of fusion (ΔH, J/g), weight fractional bulk crystallinities (ω_c), and weight fractional PCL crystallinities (X_c, per unit weight of PCL) of the PCL/PVC blends following nonisothermal treatments at a cooling rate of 0.5 °C/min from 90 to 30 °C in the absence or presence of supercritical CO_2 at 304 atm

PCL/PVC	without CO_2 treatment				with CO_2 treatment			
	T_{m1}, °C	ΔH_1, J/g	ω_{c1}, %	X_{c1}, %	T_{m2}, °C	ΔH_2, J/g	ω_{c2}, %	X_{c2}, %
100/0	59.5	74.3	52.3	52.3	57.8	82.9	58.4	58.4
90/10	58.5	65.3	46.0	51.1	56.9	72.1	50.8	56.4
75/25	55.9	50.2	35.3	47.1	55.1	57.2	40.3	53.7

by a single composition-dependent T_g observed in the DMA tangent delta curves of the blends (the figure is not shown in this report). The composition variation of T_g was from about −55 °C for pure PCL to about −40, −15, and 10 °C for the blend containing 10, 25, and 40 wt % of PVC, respectively.

Table I lists the DSC data of all samples having been crystallized by cooling from 90 to 30 °C at −0.5 °C/min. Without the presence of CO_2, the melting temperature of the nonisothermally crystallized PCL is 59.5 °C, which is depressed by PVC to 58.5 and 55.9 °C for 10 and 25 wt % of PVC incorporation, respectively. At a given composition, the blends exhibit lower melting temperatures after the crystallization under supercritical CO_2. This indicates that the PCL crystallites formed under the influence of supercritical CO_2 are thinner than those generated without the presence of CO_2, as will be further verified by the following SAXS results.

Figure 2 shows the Lorentz-corrected SAXS profiles in absolute intensity unit of the nonisothermally crystallized PCL/PVC samples without and with CO_2 treatment. For the samples without CO_2 treatment, the scattering peak is found to shift to higher q with increasing PVC content (Figure 2a), indicating that the long periods (L) associated with the lamellar stacks decreased. In the lamellar stack model with sharp phase boundary, the long period represents the sum of the crystal thickness (l_c) and the amorphous layer thickness (l_a). Decrease in long period may thus stem from the thinning of the crystal layer and/or the amorphous layer. The one-dimensional (1-D) correlation function is utilized here to reveal the composition dependences of l_a and l_c.[8,9] The 1-D correlation function, $\gamma(z)$, is given by:[13]

$$\gamma(z) = \frac{\int_0^\infty I(q)q^2 \cos(qz)dq}{\int_0^\infty I(q)q^2 dq} \quad (1)$$

where $I(q)$ is the scattering intensity obtained from the SAXS measurement and z is the direction normal to the lamellar interface.

Figure 3 shows one-dimensional correlation functions of the nonisothermally crystallized PCL/PVC blends without CO_2 treatment. The thickness of the thinner layers (l_1) of the lamellar stacks is given by the intersection between the straight line extended from the self-correlation triangle and the baseline.[9] The average thickness of the thicker layer is then

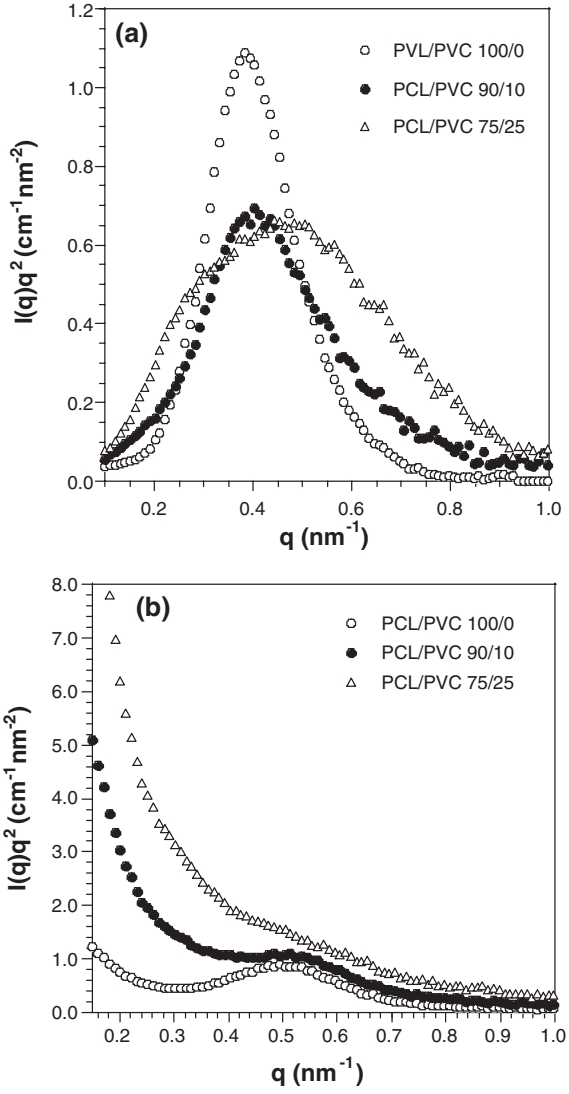

Figure 2. Lorentz-corrected SAXS profiles of PCL/PVC blends following nonisothermal treatments at a cooling rate of 0.5 °C/min from 90 to 30 °C in the absence (a) or presence (b) of supercritical CO_2 at 304 atm.

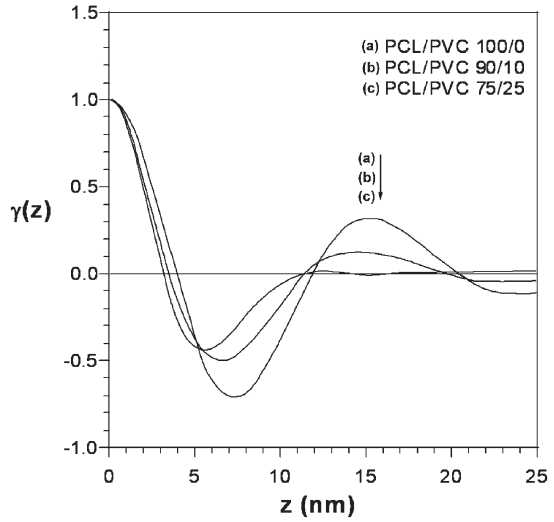

Figure 3. One-dimensional correlation functions of PCL/PVC blends following nonisothermal treatments at a cooling rate of 0.5 °C/min from 90 to 30 °C in the absence of supercritical CO_2.

given by $l_2 = L - l_1$. The l_1 and l_2 can be assigned to l_a and l_c, respectively, according to the previous SAXS studies of PCL blends.[14–18]

The values of l_c, l_a, and L obtained from Figure 3 are tabulated in Table II. It can be seen that l_a in the blends is about 1.2–1.8 nm thinner than that in neat PCL, implying that at least a portion of PVC was expelled out of the interlamellar region upon PCL crystallization. This is different from the previous studies showing that PVC was located primarily in the interlamellar regions as evidenced from the larger l_a for the blends.[19–22] The PCL/PVC blends studied previously were crystallized isothermally for a period of time. In the present study, however, the blends were crystallized through a nonisothermal crystallization process with slow cooling. According to Keith and Padden,[23] the distance over which the uncrystallizable impurity may be segregated is determined by the interplay between the diffusion coefficient (D) of impurity molecules and the crystal growth rate (G). If the diffusion rate of diluent is relatively slow compared to the crystal growth rate, the diluent molecules may be trapped inside the interlamellar regions. If the diffusion rate of the diluent is faster than the crystal growth rate, extralamellar segregation is generated. The interplay between D and G is defined by the parameter, $\delta = D/G$. δ has the unit of length and thus provides a qualitative measure of segregation distance. δ may depend on the composition, temperature, molecular weight, and polymer-polymer interaction of a blend. The extralamellar segregation observed here for the nonisothermal crystallization of PCL/PVC blends may be mainly attributed to the slower crystallization rate in the cooling process than that in the isothermal process conducted in the previous studies.

The SAXS profiles of the blends crystallized under supercritical CO_2 were drastically different from those of the samples without the treatment. As can be seen in Figure 2b, the Lorentz-corrected intensities exhibit strong upturns in the low-q region for all three samples. Instead of a simple peak, the intensity profiles are now characterized by the superposition of a monotonically decayed profile and a peak associated with the lamellar stacks. The large low-q intensity or "zero-angle scattering" signifies the presence of a heterogeneity having the characteristic size larger than that of the crystalline and amorphous layers. The intensity associated with this large-scale heterogeneity is modeled by the Debye–Bueche random structured two-phase model.[24–26] In this case, the total scattering intensity is given by

$$I(q) = \frac{A}{(1 + a_c^2 q^2)^2} + I_{LS}(q) \qquad (2)$$

The first term on the right side is the Debye–Bueche equation[27,28] with A being a constant and a_c being the correlation length characterizing the size of the large-scale heterogeneity. The second term, $I_{LS}(q)$, signifies the intensity associated with the lamellar stacks. Assuming that the low-q intensity is dominated by the Debye–Bueche equation, the correlation length associated with the large-scale heterogeneity can then be determined from the slope and intercept of the corresponding $I^{-1/2}$ *vs.* q^2 plot *via* $a_c = (\text{slope}/\text{intercept})^{1/2}$. Figure 4 shows the Debye–Bueche plots of the nonisothermally crystallized PCL/PVC blends under CO_2 treatments at 304 atm. Good linearity is

Table II. The volume fractional bulk crystallinities (ϕ_c, %), long periods (L, nm), amorphous layer thickness (l_a, nm), crystal layer thickness (l_c, nm), and correlation lengths (a_c, nm) of the PCL/PVC blends following nonisothermal treatments at a cooling rate of 0.5 °C/min from 90 to 30 °C in the absence or presence of supercritical CO_2 at 304 atm

PCL/PVC	without CO_2 treatment				with CO_2 treatment				
	ϕ_{c1}	L_1 (nm)	l_{a1} (nm)	l_{c1} (nm)	ϕ_{c2}	L_2 (nm)	l_{a2} (nm)	l_{c2} (nm)	a_c (nm)
100/0	49.7	15.4	6.0	9.4	55.9	12.1	4.9	7.2	13.8
90/10	43.4	14.6	4.8	9.8	48.2	11.3	4.6	6.7	15.2
75/25	33.0	12.4	4.2	8.2	37.8	12.2	4.9	7.3	16.3

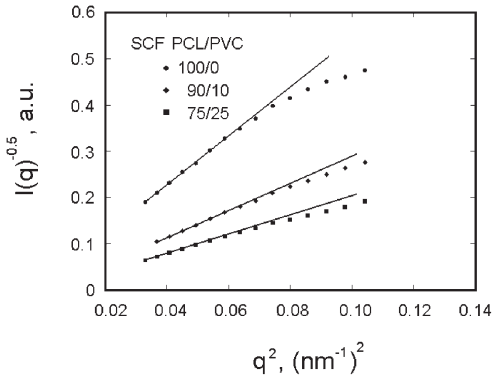

Figure 4. Debye–Bueche plots of nonisothermally crystallized PCL/PVC blends at a cooling rate of 0.5 °C/min from 90 to 30 °C under supercritical CO_2 at 304 atm.

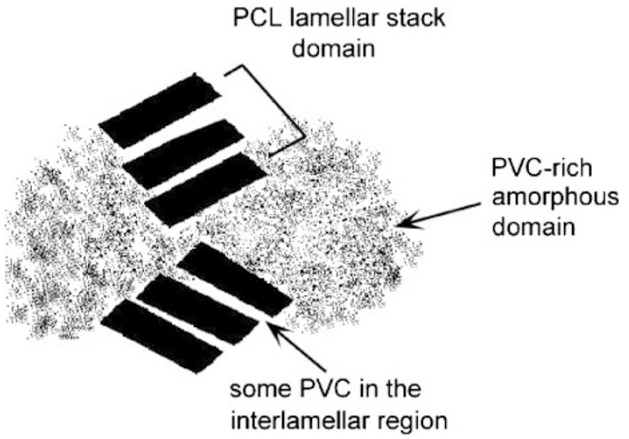

Figure 5. Schematic representation of heterogeneous morphology of the nonisothermally crystallized PCL/PVC blends under supercritical CO_2 treatments at 304 atm at a cooling rate of 0.5 °C/min from 90 to 30 °C.

observed in the low-q region, whereas deviation from the initial linearity at higher q region due to the contribution of the scattering associated with the lamellar stacks. The correlation lengths deduced from Figure 4 are 13.8, 15.2 and 16.3 nm for PCL/PVC = 100/0, 90/10, and 75/25, respectively (Table II), showing that the size of the large-scale heterogeneity increases with increasing PVC content.

According to Schultz,[29] the zero-angle scattering exhibited by semicrystalline polymers may be attributed to the presence of large (greater than lamellar length scales) individual amorphous domains located between the lamellar bundles so as to generate gaps in the sequential stacking of lamellae. In the case of PCL/PVC blends, it appears that the supercritical CO_2 treatment promotes the segregation of PVC out of the interlamellar regions, where the expelled PVC chains form large amorphous domains located between the lamellar bundles (as schematically represented in Figure 5) and consequently gives rise to the stronger zero-angle scattering.

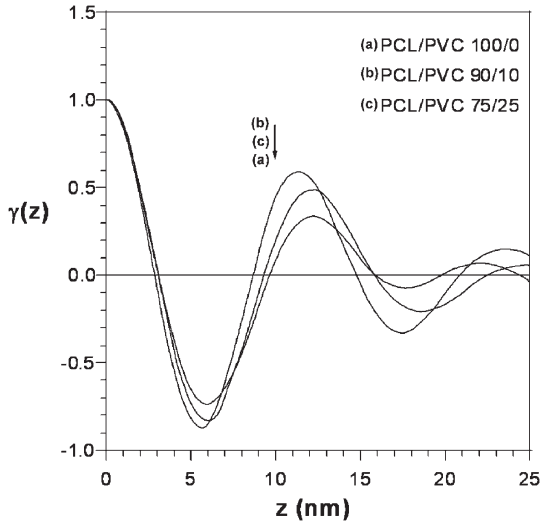

Figure 6. One-dimensional correlation functions of PCL/PVC blends following nonisothermal treatments at a cooling rate of 0.5 °C/min from 90 to 30 °C in the presence of supercritical CO_2 at 304 atm. The correlation functions were calculated by the scattering intensities stemming from the lamellar stacks, $I_{LS}(q)$, which were obtained by subtracting the intensity from the large-scale heterogeneity from the observed intensity profile in Figure 2b.

According to eq 2, the scattering intensity stemming from the lamellar stacks, $I_{LS}(q)$, may be obtained by subtracting the intensity from the large-scale heterogeneity (described by the Debye–Bueche equation) from the observed intensity profile. The resultant $I_{LS}(q)$ can then be used to calculate $\gamma(z)$ from which l_a, l_c and L of the CO_2-treated blends are determined. Figure 6 shows one-dimensional correlation functions obtained through this procedure. The corresponding values of l_a, l_c and L are also listed in Table II. For a given blend composition, the thickness of crystal layer is found to decrease after nonisothermal crystallization under supercritical CO_2 treatments. This is consistent with the T_m data as measured by DSC, showing that the melting point depresses upon CO_2 treatment. According to the secondary nucleation theory, at low to moderate degree of supercooling, the initial crystal thickness (l_g^*) is given by:[30,31]

$$l_g^* \cong \frac{2\sigma_e T_m^0}{\Delta h_f^0 (T_m^0 - T_c)} \tag{3}$$

where σ_e is the fold surface free energy, T_m^0 is the equilibrium melting point, Δh_f^0 is the bulk enthalpy of melting per unit volume, and T_c is the crystallization temperature. The final crystal thickness, according to the notation of Hoffman and Weeks,[30,31] is γ times the initial thickness, namely,

$$l_c = \gamma l_g^* \tag{4}$$

where γ is the so-called "lamellar thickening factor".

Since T_m^0, T_c, and Δh_f^0 are constant for a blend in this work, the decrease in l_c under supercritical CO_2 treatment suggests that the σ_e is lower in CO_2 as compared with that in air.

To gain further insight into the extent of extralamellar segregation of PVC upon PCL crystallization in the blends, the electron density contrast, $\Delta\eta$, between the crystalline and amorphous layers in the lamellar stacks are calculated from the absolute scattering intensity. Because the electron density of PVC is significantly higher than that of PCL, incorporation of PVC in the interlamellar region is expected to enhance $\Delta\eta$. The scattering invariant (Q) can be determined from the absolute intensity *via*

$$Q = \frac{1}{2\pi^2}\int_0^\infty I(q)q^2dq \tag{5}$$

For a two-phase model, the invariant is related to the electron density contrast by[13]

$$Q = \phi_s\phi_{cs}(1-\phi_{cs})\Delta\eta^2 \tag{6}$$

where ϕ_{cs} is the crystallinity within the lamellar stacks (or linear crystallinity) given by

$$\phi_{cs} = \frac{l_c}{L} \tag{7}$$

ϕ_{cs} is related to the volume fractional bulk crystallinity, ϕ_c, by

$$\phi_c = \phi_s\phi_{cs} \tag{8}$$

where ϕ_s is the volume fraction of lamellar stacks in the sample and thus is given by ϕ_c/ϕ_{cs} from eq 8. ϕ_c, as tabulated in Table II, is calculated from weight fraction of crystallinity (ω_c) measured by DSC. $\Delta\eta$ can then be calculated by eq 6 with the knowledge of Q, ϕ_{cs}, and ϕ_c. Table III tabulates the $\Delta\eta$ values obtained from the measured invariant of blends both without and with CO_2 treatments. $\Delta\eta_{msd.1}$ and $\Delta\eta_{msd.2}$ are used to denote those measured $\Delta\eta$ values for without and with CO_2 treatments, respectively. The plots of $\Delta\eta_{msd.1}$ and $\Delta\eta_{msd.2}$ as a function of w_{PVC} are shown in Figure 7.

As can be seen in Table III for neat PCL, the measured electron density contrast $\Delta\eta_{msd.1}$ is 0.050 (mol electrons/cm^3), which is close to the value of 0.0464 obtained by subtracting 0.5928 (mol electrons/cm^3) for amorphous PCL from 0.6392 (mol electrons/cm^3) for crystalline PCL. These calculated electron densities were calculated from mass densities of 1.1753 and 1.09 g/cm^3 for crystalline and amorphous PCL, respectively.[32] The measured electron density contrasts $\Delta\eta_{msd.1}$ of the blends are larger than that of neat PCL, indicating that some PVC is still located in the interlamellar region after PCL crystallization. By contrast, it can be seen that the electron density contrasts of the blends with CO_2 treatment, $\Delta\eta_{msd.2}$, are nearly the same as that of neat PCL. This indicates that nearly all PVC was expelled out of the interlamellar regions upon PCL crystallization under supercritical CO_2. Therefore, the CO_2 treatment promotes the segregation of PVC out of the interlamellar region presumably due to the significant enhancement of the chain mobility of PVC by lowering its T_g. This is indeed consistent with the stronger zero-angle scattering observed for the CO_2-treated blends in Figure 2b, where the PVC chains segregated out of the interlamellar regions form large amorphous domains between the lamellar bundles (Figure 5) to give rise to the strong intensity upturn at low q.

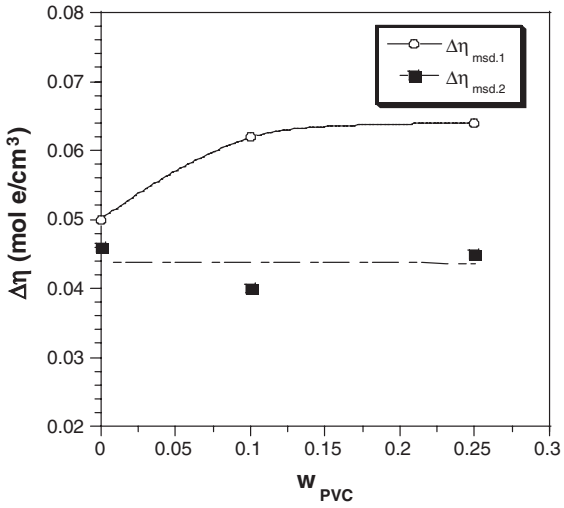

Figure 7. Comparison between composition variation of the measured $\Delta\eta$ ($= \eta_c - \eta_a$) values for PCL/PVC blends following nonisothermal treatments at a cooling rate of 0.5 °C/min from 90 to 30 °C in the absence ($\Delta\eta_{msd.1}$) and presence ($\Delta\eta_{msd.2}$) of supercritical CO_2 at 304 atm.

Table III. The measured $\Delta\eta$ ($= \eta_c - \eta_a$) values of PCL/PVC blends following nonisothermal treatments at a cooling rate of 0.5 °C/min from 90 to 30 °C in the absence ($\Delta\eta_{msd.1}$) or presence ($\Delta\eta_{msd.2}$) of supercritical CO_2 at 304 atm

PCL/PVC	$\Delta\eta_{msd.1}$ (mol e/cm^3)	$\Delta\eta_{msd.2}$ (mol e/cm^3)
100/0	0.050	0.046
90/10	0.062	0.040
75/25	0.066	0.045

CONCLUSIONS

Nonisothermal crystallizations of compatible crystalline/amorphous PCL/PVC blends under supercritical CO_2 at 304 atm from 90 °C (above melting temperature of PCL) to 30 °C could lead to decreases in thickness of the crystalline layers in the lamellar stacks as compared with those without the presence

of supercritical CO_2. In addition, a large-scale heterogeneity with the size larger than the crystalline and amorphous layer thickness was found in the CO_2-treated blends. This heterogeneity was attributed to the amorphous domains formed by the PVC chains that were expelled out of the interlamellar regions upon PCL crystallization. The CO_2 treatment promoted the segregation of PVC out of the interlamellar region presumably due to the significant enhancement of the chain mobility of PVC by lowering its T_g.

Acknowledgment. We thank National Science Council of Republic of China for financial support for this work.

REFERENCES

1. C. Lepilleur and E. J. Beckman, *Macromolecules*, **30**, 745 (1997).
2. J. L. Kendall, D. A. Canelas, J. L. Young, and J. M. DeSimone, *Chem. Rev.*, **99**, 543 (1999).
3. B. Baradie and M. S. Shoichet, *Macromolecules*, **35**, 3569 (2002).
4. D. L. Tomasko, H. Li, D. Liu, X. Han, M. J. Wingert, L. J. Lee, and K. W. Koelling, *Ind. Eng. Chem. Res.*, **42**, 6431 (2003).
5. C. F. Kirby and M. A. McHugh, *Chem. Rev.*, **99**, 565 (1999).
6. Z. Zhang and Y. P. Handa, *Macromolecules*, **30**, 8505 (1997).
7. J. J. Watkins, G. D. Brown, V. S. RamachandraRao, M. A. Pollard, and T. P. Russell, *Macromolecules*, **32**, 7737 (1999).
8. Y.-T. Shieh, Y.-G. Lin, and H.-L. Chen, *Polymer*, **43**, 3691 (2002).
9. Y.-T. Shieh, K.-H. Liu, and T.-L. Lin, *J. Supercrit. Fluids*, **28**, 101 (2004).
10. Y.-T. Shieh and H.-S. Yang, *J. Supercrit. Fluids*, **33**, 183 (2005).
11. B. Wunderlich, "Macromolecules Physics" vol. 3, Academic Press, New York, 1980.
12. G. Defieuw, G. Groeninckx, and H. Reynaers, *Polymer*, **30**, 595 (1989).
13. G. R. Strobl and M. Schneider, *J. Polym. Sci., Polym. Phys. Ed.*, **18**, 1343 (1980).
14. T. P. Russell and R. S. Stein, *J. Polym. Sci., Polym. Phys. Ed.*, **21**, 999 (1983).
15. M. Vanneste, G. Groeninckx, and H. Reynaers, *Polymer*, **38**, 4407 (1997).
16. H.-L. Chen, S. Wang, and T. Lin, *Macromolecules*, **31**, 8924 (1998).
17. S.-W. Kuo, S.-C. Chan, and F.-C. Chang, *J. Polym. Sci., Part B: Polym. Phys.*, **42**, 117 (2004).
18. B. Zhu, Y. He, N. Yoshie, N. Asakawa, and Y. Inoue, *Macromolecules*, **37**, 3257 (2004).
19. R. S. Stein, F. B. Khambatta, F. P. Warner, T. Russell, A. Escala, and E. Balizer, *J. Polym. Sci., Polym. Symp.*, **63**, 313 (1978).
20. M. Canetti, P. Sadocco, A. Siciliano, and A. Seves, *Polymer*, **35**, 2884 (1994).
21. C. J. Ong and F. P. Price, *J. Polym. Sci., Polym. Symp.*, **63**, 45 (1978).
22. G. Defieuw, G. Groeninckx, and H. Reynaers, *Polymer*, **30**, 2164 (1989).
23. H. D. Keith and F. J. Padden, *J. Appl. Phys.*, **35**, 1270 (1975).
24. S. Nojima, Y. Terashima, and T. Ashida, *Polymer*, **27**, 1007 (1986).
25. S. Nojima, K. Satoh, and T. Ashida, *Macromolecules*, **24**, 942 (1991).
26. H.-L. Chen and M. S. Hsiao, *Macromolecules*, **31**, 6579 (1998).
27. P. Debye and A. M. Bueche, *J. Appl. Phys.*, **20**, 518 (1949).
28. P. Debye, H. R. Anderson, Jr., and H. Brumberger, *J. Appl. Phys.*, **28**, 679 (1957).
29. J. M. Schultz, *J. Polym. Sci., Part B: Polym. Phys.*, **14**, 2291 (1976).
30. J. D. Hoffman and J. J. Weeks, *J. Res. Natl. Bur. Stand.*, **66A**, 13 (1962).
31. J. D. Hoffman and R. L. Miller, *Polymer*, **38**, 3151 (1997).
32. J. Brandrup and E. H. Immergut, "Polymer Handbook," 3rd ed., John Wiley & Sons, New York, 1989.